

Experimental Validation of the Mathematical Model for a Recirculating Solar Dryer

N. M. Nazarova^{a,*}, M. R. Nazarov^b, and T. D. Juraev^a

^a Bukhara State University, Bukhara, Uzbekistan

^b Pedagogical Institute, Bukhara State University, Bukhara, Uzbekistan

*e-mail: nazarova_nargiza85@mail.ru

Received November 17, 2021; revised January 6, 2022; accepted June 1, 2022

Abstract—Data are provided on studying the development of effective solar energy dryers and the spheres of their practical application are considered. An energy-saving recirculating solar energy dryer with a recuperative heat exchanger is developed for drying produce with a fresh product load volume of 30 kg. A mathematical model for the drying processes in the suggested recirculating solar energy dryer is also presented. The experimental verification of the mathematical model of the recirculating solar drying installation is presented. The diurnal variations in the ambient temperature and heat flux density of incident total solar radiation were used as the input data; the tests were conducted in the city of Bukhara. The results of the statistical analysis of the diurnal variations in the temperature inside the solar dryer show good agreement. Also, an experimental verification of the known models for apple drying in a recirculating solar dryer and in open air are presented. Among these models, the Henderson and Pabis model showed the best fit between calculated and experimental results. This allows us to carry out full-scale calculations in solar dryers using the Henderson and Pabis drying model.

Keywords: validation, solar dryer, recirculation, mathematical model

DOI: 10.3103/S0003701X2202013X

INTRODUCTION

It is known that drying agricultural products in solar plants has certain economic advantages to drying in open sites. However, drying in the open air has still been widely used in most developing countries. Produce is mostly dried on the ground, concrete, and even on the roads under the sun's rays [1]. Besides, such drying under certain climate conditions leads to loss of quantity and quality of the final product [2]. According to the estimates for developing countries, the general postharvest losses account for up to 50%; sometimes up to 40% of the harvest does not reach customers due to postharvest losses in the supply chain [4].

During solar drying, solar energy is used either as the main or additional source of heat. The flux of a drying agent (heated air) can be controlled by natural or forced convection, while the preheated air can pass through a product without exposure of direct solar radiation or direct effect of solar radiation. Both regimes can be combined [5]. Several criteria, such as characteristics of product drying, the requirements to the quality, and expenses for drying determine the final choice of solar dryers [6, 7].

Solar dryers vary from very primitive, being used in small distant populated areas, to more complicated industrial installations. Although, the latter are still only a few, they are at the stage of development. It is not an easy task to finally classify solar dryers since they are configured differently, many configurations are empirical. They can be classified by different criteria, e.g., by the type of dryer; the operating temperature or a drying material; the operation regime, e.g., periodic or continuous, etc. Study [8] presents systematic classification based on the structure and way of using solar energy. All developed solar dryers are divided into chamber (convective), solar radiation, and combined by their design features and principles of operation [9–11].

Study [12] reviews the different designs and principles of operation for a wide range of solar driers. It also provides a full classification of solar dryers. Depending on the drying process (direct or indirect), they can be passive dryers heated directly from solar radiation with or without natural air circulation and active solar dryers (with forced convection) where a ventilator circulates the drying agent [13]. Despite numerous configurations of active solar dryers with forced circulation, they consist of almost the same components [13]:

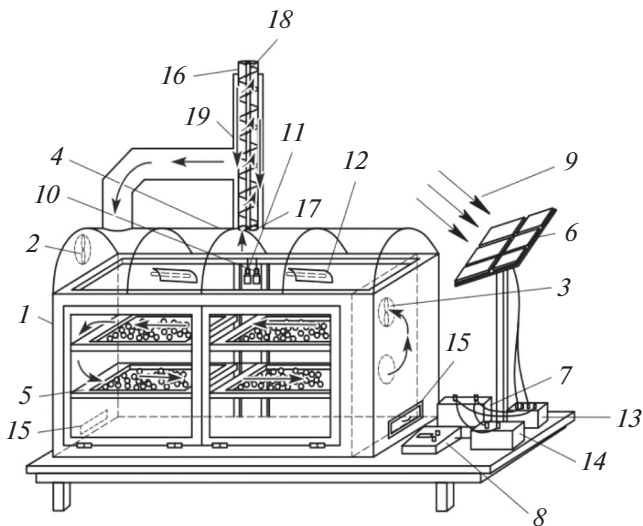


Fig. 1. The schematic of the recirculating solar dryer (RSD): (1) drying chamber; (2) exhaust ventilator 1 (for discharge of humid air); (3) ventilator 2 (for active ventilation); (4) transparent insulation; (5) drying trays for products; (6) solar cell (SC); (7) electric battery; (8) CP (control panel); (9) solar rays; (10) temperature sensor; (11) air humidity sensor; (12) IR lamps; (13) controller; (14) inverter; (15) ventilation window; (16) exhaust tube; (17) exhaust ventilator; (18) screw device; (19) recuperative heat exchanger.

chamber, tunnel, etc., are used as a space for dried material, e.g., a solar collector is employed as a heating system for the drying agent; the ventilators are used as recirculating systems of the drying agent, etc.

The comprehensive reviews of the structures of solar dryers were given in [13–21]. The integrated review of the structure of solar dryers for indirect drying of different products was given in [22]. Studies [23, 27] overviewed the solar dryers designed for drying grapes. In [24], the combined solar dryer is offered for drying mushrooms using materials with a phase transition. We note that in recent years, researchers have begun developing combined solar dryers (radiation-convective) for produce that operate on forced circulation of a drying agent [25–27]. However, such installations are stationary and are intended for drying large volumes of produce. The broad development of private farms producing different agricultural products requires simplified mobile variants of solar drying installations that do not need large capital and operating expenses and can be installed during the drying season at the places of direct production of agricultural products [28, p. 5].

Our study presents experimental validation of the mathematical model for the recirculating solar drying installation. In addition, we performed calculations for the validation of the presented model and com-

pared the calculated and the experimental results. As initial data, we used diurnal variations in the ambient temperature and heat flux density of the incident total solar radiation. The results of statistical analysis of diurnal variations in the temperature inside the solar dryer show good agreements.

MATERIALS AND METHODS

To intensify and increase the efficiency of the drying process, we designed a solar dryer with a recuperative heat exchanger for produce with a fresh product load volume of 30 kg, having a transparent surface with an area of 6 m² [38]. The schematic of the proposed solar dryer is presented in Fig. 1.

The solar dryer contains a drying chamber equipped with a ventilation system (2, 3, 17) and control panel (8) with a self-contained power supply. The drying chamber is rectangular with a size of 2.0 × 0.80 × 1.30 m³ has arc-shaped transparent upper cover (4), and mesh trays (5) for a dried product. The dryer and the air heater are combined in one chamber. The mesh trays are placed in the drying chamber stagewise, the distance between them was selected with respect to the creation of a uniform flux of a heat carrier. The trays with a metal mesh bottom have a rectangular shape with a size of 0.80 × 0.80 × 0.05 m³. The dryer holds four trays with a total area of 1.80 m². The top and lateral parts of the dryer are covered with transparent sheets of cellular polycarbonate 6 mm thick and are hermetically sealed, since this material decreases thermal losses by a factor of 2–3 compared to window glass. To fill in fresh portions of produce, the front part of the drying chamber has tightly closed doors.

Exhaust pipe (16) is installed in the upper part of the dryer to remove the exhaust drying agent. The exhaust pipe is constructed so that it is also used as a recuperative heat exchanger–heat utilizer (19) (RHU). The RHU consists of internal and external tubes (tube in tube) and the exhaust ventilator. The height of the internal tube is 2 m and inside is screw device (18). The diameters of the RHU internal and external tubes are 20 cm and 16 cm, respectively. The external tube of the RHU is black in color, which is heated during the daytime due to solar radiation (Fig. 1).

The principle of RHU operation is the following. During the process of produce drying, the spent drying agent is discharged to the atmosphere by exhaust ventilator (17) through the screw channel. While moving, the spent drying agent gives out a part of its heat to the atmospheric air coming into the heat exchanger from the outside through the walls of the screw pipe. The external tube of the recuperative heat exchanger is heated due to solar radiation absorption and gives out

a part of its heat to the air flow coming into the dryer (Fig. 1). The flow of the currents in the internal and external channels can be taken as countercurrent since the countercurrent recuperative heat exchange is the most effective [39]. Hence, this measure with the use of RHU ensures additional heating of the internal air of the chamber in drying the produce by recuperating the heat of the spent heat carrier.

The automatic control unit with self-contained power supply consists of solar module (6), electric battery (7) and control panel (8). The solar panel is mounted on a special holder near the drying chamber. The solar cell output voltage is supplied to the controller from which electric energy is accumulated in electric battery. (Fig. 1.) A KGT-500 infrared radiator (infrared lamp) was used as an additional source of heat in the drying chamber, equipped with solar powered reflector (12) (2 items).

The offered dryer can operate in the regimes of forced circulation and recirculation. In the regime of circulation, the dryer operates as follows: after being loaded with produce, the dryer closes in the lower part of the small window and ventilator (2) (exhaust ventilator (2) serves for removal of a gas–vapor mixture from the drying chamber) turns off. The air heated to 55–60°C passes by blower fan (3) through the produce and the process of drying begins. In the first period of drying, the moisture content of the air in the chamber gradually increases. As soon as the established value of relative air humidity is reached inside the chamber, humidity sensor (11) (DHT-21 type) automatically actuates exhaust ventilator (17). Then, with a decrease in air humidity in the chamber to the assigned value, a signal from humidity sensor (17) switches off exhaust ventilator (17), and the process repeats.

Modeling of a Solar Dryer

Modeling of solar drying is a much more complicated process compared to ordinary drying where a product is blown over by hot air. Modeling of a principle of solar dryer operation gets complicated due to the following phenomena: (1) fluctuations in incident radiation and environmental conditions (temperature, relative humidity); (2) phenomenon of partial rehydration of a product during the nighttime); and (3) the use of auxiliary systems of heating or an air flow and accumulation of thermal energy that are employed to soften the variations in the environment parameters and to ensure continuous operation [29–30]. In addition, a decisive role is also played by thermal and mass-exchange with a turbulent air flow across a boundary layer in addition to the processes of transport inside the dried material.

We note that the main purpose of the study is to improve the efficiency of dryers and to obtain high-quality dry products due to sustainable use of alternative energy sources, as well as to analyze the recent technology of solar drying.

Mathematical Model of a Solar Dryer

The heat balance equation for the product inside the drying chamber [31] will be

$$C_{pr}M_{pr}\frac{dT_{pr}}{dt} = \alpha_{conv1}(T_a - T_{pr})S_{pr} - (\alpha_{conv2} + \alpha_{evap})(T_{pr} - T_{h,air})S_{pr} + \alpha_{pr}S_{pr}q_{incid}^{\Sigma}, \quad (1)$$

where C_{pr} , M_{pr} , and T_{pr} are the specific heat, mass, and temperature of a product, respectively; α_{conv1} is the convective heat transfer coefficient from the product in hot air; α_{conv2} and α_{evap} are evaporative and convective heat transfer coefficients from the product in humid air; S_{pr} is the surface area of the product T_a is the temperature of the incoming hot air; $T_{h,air}$ is the temperature of humid air; α_{pr} is the coefficient of ray absorption of the product; q_{incid}^{Σ} is incident total solar radiation; and t is the time.

The heat balance equation for humid air in the drying chamber will be:

$$C_{h,air}M_{h,air}\frac{dT_{h,air}}{dt} = (\alpha_{conv2} + \alpha_{evap})(T_{pr} - T_{h,air})S_{pr} - \alpha_{conv3}(T_{h,air} - T_{wall})S_{wall} - c_d S_e \sqrt{2g\Delta H\Delta P}, \quad (2)$$

where $C_{h,air}$, $M_{h,air}$, and $T_{h,air}$ are the specific heat, mass, and temperature of humid air; c_d is the coefficient of discharge of the drying facility; S_e is the exit hole surface; α_{conv3} is the convective heat transfer coefficient from the wall of the facility in humid air; S_{wall} is the wall surface area; and g is the acceleration of gravity.

The changes in head ΔH (m) and partial pressure ΔP (N/m²) are expressed as [32]:

$$\Delta H = \frac{\Delta P}{\rho_{air}g}, \quad (3)$$

$$\Delta P = P(T_{h,air}) - \gamma P(T_{amb}), \quad (4)$$

$$P(T) = \exp\left(25.317 - \frac{5144}{T + 273.15}\right), \quad (5)$$

where ρ_{air} is the humid air density; γ is the psychrometric constant; P is the partial pressure of the study medium (humid air inside the chamber, outer air);

The heat balance equation for the wall of the drying chamber:

$$C_{\text{wall}} M_{\text{wall}} \frac{dT_{\text{wall}}}{dt} = \alpha_{\text{conv}3} (T_{\text{h.air}} - T_{\text{pr}}) S_{\text{wall}} - \alpha_d (T_{\text{wall}} - T_{\text{amb}}) S_{\text{wall}}, \quad (6)$$

where C_{wall} , M_{wall} , T_{wall} , and S_{wall} are the specific heat, mass, temperature, and surface area of the wall, respectively; α_d is the heat transfer coefficient from the wall in the medium; and T_{amb} is the ambient temperature.

To predict the efficiency of the system, instantaneous thermal efficiency of the dryer takes on form

$$\eta = \frac{\alpha_{\text{evap}} (T_{\text{pr}} - T_{\text{h.air}})}{q_{\text{incid}}} \times 100. \quad (7)$$

The convective heat transfer coefficient from the produce in hot air is written as

$$\alpha_{\text{conv}1} = \alpha_{\text{conv}2} = \text{Nu} \frac{\lambda_{\text{air}}}{D}. \quad (8)$$

For the turbulent flow:

$$\text{Nu} = 0.023 \text{Re}^{0.8} \text{Pr}^{0.4}, \quad (9)$$

$$0.7 \leq \text{Pr} \leq 120, \quad 10^4 \leq \text{Re} \leq 1.2 \times 10^5.$$

Reynolds number is expressed as:

$$\text{Re} = \frac{U_a l}{\vartheta}. \quad (10)$$

For the turbulent flow:

$$\text{Nu} = 0.036 \text{Re}^{0.8} \text{Pr}^{0.33}, \quad (11)$$

$$\text{Pr} \geq 0.5, \quad \text{Re} > 5 \times 10^5, \quad (12)$$

where Nu is the Nusselt number; Pr is the Prandtl number; Re is Reynolds number; λ_{air} is the heat conduction coefficient of humid air; D is the typical diameter of the product layer; U_a is the air velocity; l is the typical size; and ϑ is kinematic viscosity of humid air.

The insulation thermal conductivity coefficient is calculated by formula:

$$\alpha_d = \frac{\lambda_i}{d_i}, \quad (13)$$

where λ_i and d_i is the thermal conductivity coefficient and the thickness of the study insulation layer, respectively.

The evaporative heat transfer coefficient equals

$$\alpha_{\text{evap}} = 0.016 \alpha_{\text{conv}1} \frac{[P(T_{\text{pr}}) - \gamma P(T_{\text{h.air}})]}{T_{\text{pr}} - T_{\text{h.air}}}. \quad (14)$$

To solve differential Eqs. (1)–(6) with boundary conditions presented in Fig. 1, we used the Laplace transform method (operation method).

Moisture Content

The moisture content in the product can be expressed either on a wet basis (M_{wb}) or on a dry basis (M_{db}) of substance (either in a decimal or in percentage). Moisture content on a wet basis (M_{wb}) is the weight of moisture (M_w) in the product per unit weight of undried material (M_0), which is found as

$$M_{\text{wb}} = \frac{M_w}{M_0} = \frac{M_w}{M_w + M_d}, \quad (15)$$

While moisture content on a dry basis is the weight of moisture (M_w) in the product per unit weight of dry material (M_d) and is calculated as

$$M_{\text{db}} = \frac{M_w}{M_d} = \frac{M_w}{M_0 - M_w}. \quad (16)$$

Moisture contents on a wet basis (M_{wb}) and on a dry basis (M_{db}) are correlated in accordance with equations:

$$M_{\text{wb}} = 1 - \left[\frac{1}{(M_{\text{db}} + 1)} \right], \quad (17)$$

$$M_{\text{db}} = \left[\frac{1}{(1 - M_{\text{wb}})} \right] - 1. \quad (18)$$

Drying Kinetics

Drying kinetics shows the time changes in the average moisture content and the average temperature in the product, while drying dynamics describes the changes in the temperature and moisture profiles for the whole product. By knowing the drying kinetics, we can use it in calculating the amount of evaporated moisture, the time of drying, power consumption, and other related parameters, which is very important, since it is used in designing and modeling the dryer [34]. In addition, drying kinetics fully explains the properties of transfer, such as mass transfer coefficient, moisture diffusion, heat transfer, etc., involved in the process of drying.

Drying kinetics can be determined as the dependence of factors affecting drying and the rate of drying. Moisture transfer during drying can be described by using first-order kinetic model

$$-\frac{dM}{dt} = k(M - M_e), \quad (19)$$

where: M is the moisture content in the material (on a dry basis) during drying (kg of water/kg of dry substances); M_e is the moisture equilibrium in the dried material (kg of water /kg of dry substances); k is the rate of drying (s^{-1}); and t is the drying time (s).

The rate of drying is related to the humid air temperature and is calculated by the following relationship:

$$k = -9.75 \times 10^{-4} + 3.29 \times 10^{-6} T_{h,air} \quad (20)$$

Consequently, moisture equilibrium is determined the following way

$$M_e = \frac{W_m C K a_w}{(1 - K a_w)[1 + (C - 1) K a_w]} \quad (21)$$

where W_m , C , and K are the parameters associated with the air temperature, which are calculated by the following expressions:

$$W_m = 0.0014254 \exp\left(\frac{1193.2}{T_{conv}}\right), \quad (22)$$

$$C = 0.5923841 \exp\left(\frac{1072.5}{T_{conv}}\right), \quad (23)$$

$$K = 1.00779919 \exp\left(-\frac{43.146}{T_{conv}}\right). \quad (24)$$

For any material, the rate of drying is determined as the slope of the drying curve with a decreasing rate. At $t = 0$, the moisture content equals the initial moisture content (i.e., $M = M_0$). We integrate the above equation to obtain the following expression for moisture content at the moment of time t and M_t :

$$M_t = M_e - (M_e - M_0) \exp(-kt). \quad (25)$$

This equation is written as

$$MR = \frac{M_t - M_e}{M_0 - M_e} \approx \frac{M_t}{M_0} = \exp(-kt). \quad (26)$$

Thin-Layer Drying

Thin-layer drying equations can be described by theoretical, semitheoretical, or empirical equations [35–37]. The theoretical models were obtained with respect to internal resistance to moisture transfer where the product behavior is explained during drying operations under any conditions. However, these models were developed with many assumptions that lead to appreciable errors. The most widely used theoretical models are based on Fick’s 2nd law of diffusion [36]. Most semitheoretical models are based on Fick’s 2nd law of diffusion and Newton’s law of cooling [35].

The models obtained from Newton’s law of cooling include

- Lewis (Newton) evaporation model [35],

$$MR = \exp(-kt) \quad (27)$$

- Page evaporation model [36],

$$MR = \exp(-kt^n). \quad (28)$$

The models obtained from Fick’s 2nd law of diffusion:

- Henderson and Pabis evaporation model [37],

$$MR = a \exp(-kt). \quad (29)$$

Mathematical Statistics of Model Verification

The accuracy of the proposed model at each level of verification and validation was estimated by using the methods of the value of coefficient of determination (R^2), mean bias error (MBE) and root-mean square error (RMSE). In general, the coefficient of determination shows how well the function correlates to the set of data. RMSE is a measure of how spread out the remainders are, which demonstrates how focused the data are around the line of best fit. The statistical analysis of the drying agent temperature calculated for the proposed mathematical model was conducted by comparing the experimental results conducted on September 5 and 6, 2020.

$$R^2 = 1 - \frac{\sum_{i=1}^N (R_{m_i} - R_{e_i})^2}{\sum_{i=1}^N \left(R_{m_i} - \frac{1}{N} \sum_{i=1}^N R_{m_i} \right)^2}, \quad (30)$$

$$MBE = \frac{1}{N} \sum_{i=1}^N (R_{m_i} - R_{e_i}), \quad (31)$$

$$RMSE = \left[\frac{1}{N} \sum_{i=1}^N (R_{m_i} - R_{e_i})^2 \right]^{\frac{1}{2}}, \quad (32)$$

where N is the number of data points and R is the data set. Subscripts e and m designate the experimental and estimated data, respectively. The values of the coefficient of determination (R^2) and root-mean-square error (RMSE) are used to determine the quality of the mathematical model of solar drying facility and drying kinetics. To evaluate the best curve of drying, we selected the largest values of R^2 and the smallest values of MBE and RMSE [33].

RESULTS AND DISCUSSION

Verification of the Mathematical Model of a Solar Dryer

To verify the validity of the proposed mathematical model, we conducted a statistical analysis where the results were compared to the experimental results obtained on September 5 and 6, 2020. Figure 2 presents the diurnal variations in the ambient temperature and the flux density of the incident total solar radiation. According to the measurement results, the maximum ambient temperature is observed at 2:00 p.m,

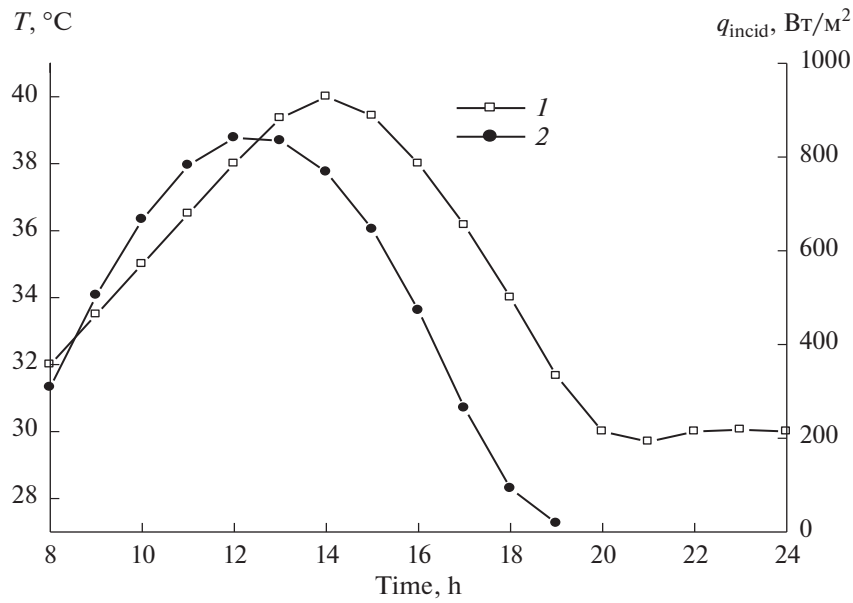


Fig. 2. Diurnal variations in (1) ambient temperature and (2) flow density, incident total solar radiation.

while the peak value of the incident total solar radiation flux density is recorded at 12:00 p.m.

As is shown by the results of the statistical analysis of the diurnal variations in the temperature inside the solar dryer, the RMSE equals 2.3°C, the RMSE in percent is equal to 5.7%, and the square of the correlation coefficient is 0.86. The main shift between the results of the experimental and calculated data is recorded at the peak temperature values.

Verifications of the Model of Drying Kinetics

The experiments on studying the drying kinetics of fruits and berries were conducted in the recirculating solar drying facility. Apples were chosen as an object of drying. Before the experiment began, the products were placed on mesh shelves without preliminary treatment. Each shelf can hold 8–10 kg of products. For the comparative analysis, we weighed a small product sample.

Table 1. Experimental measured data in open air solar drying and in chamber drying

Time of day	m_1 , g	m_2 , g	t_{amb}	Φ_1	t_1	t_2	Φ_2	t_p
10:00 a.m.	100	100	32.4	13	46	46	50	34
11:00 a.m.	92	86	34.1	10	44	44	50	36.1
12:00 p.m.	81	71	34.8	12	48	47	46	40.2
01:00 p.m.	70	56	36	12	52.3	51.3	38	43.9
02:00 p.m.	64	43	36.8	10	54.3	52.7	32	47
03:00 p.m.	54	33	37.6	10	54	53.2	25	47.6
04:00 p.m.	44	26	36.7	10	52.3	51.1	19	48.9
05:00 p.m.	37	22	36.6	10	42.8	43.1	21	42.6
10:00 a.m.	34	20	35.7	10	38.2	38.2	21	38.4
11:00 a.m.	23	17	31.4	18	48.4	53.1	21	49.2
12:00 p.m.	23	16	34.9	14	57.2	58.6	16	57.3
01:00 p.m.	22	16	36.3	12	64.7	64.7	16	57.3

Mass of produce at the open site (m_1), mass of produce in the dryer (m_2), ambient temperature (t_{amb}); outer air humidity (Φ_1); temperature of air inside the dryer in the lower part (t_1) and in the upper part (t_2), respectively; relative humidity of air inside the dryer (Φ_2); produce temperature (t_p)

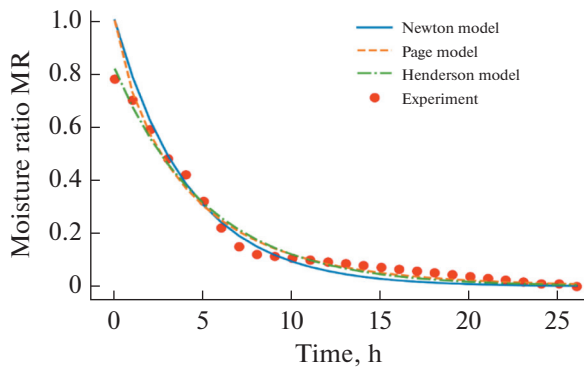


Fig. 3. Kinetics of apply drying in open air solar drying.

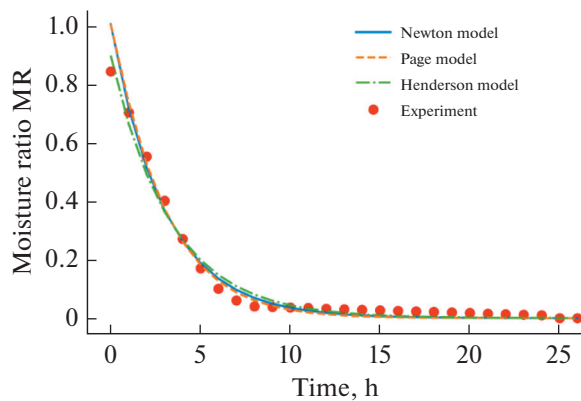


Fig. 4. Kinetics of drying in a solar drying chamber.

In the course of the experiments, we measured the following parameters: the time of the day, weight of produce at the open site; weight of produce in the drying chamber; ambient temperature; ambient air humidity; air temperature inside the drying chamber in the upper and lower parts, respectively; relative air humidity inside the drying chamber; temperature of the produce; air temperatures at the entrance of the heat exchanger; in the middle, and at the exit, respec-

tively; the relative air humidity at the entrance of the pipe; the temperature of the drying agent at the exit of the pipe; the ambient temperature of the pipe; the rate of drying agent in the upper and lower parts of the drying chamber; and the rate of heat carrier at the entrance and at the exit of the pipe (Table 1).

Figure 3 provides the estimated and experimental data on drying kinetics of apples during solar drying in open air. All theoretical, semitheoretical, and empirical equations of drying kinetics illustrate an excellent fit to the experimental results. However, the best result is shown only by the Henderson and Pabis model [35]. Table 2 shows the detailed statistical analysis of the results (regime 1 corresponds to the regime where the product sample was obtained during the solar drying in the open air).

During the solar drying of apples in the drying chamber, the estimated and empirical kinetics of product drying showed the best consistency to the theoretical, semitheoretical, empirical, and experimental results (Fig. 4). However, the best result is shown only by the Henderson and Pabis model, where the values of determination coefficient (R^2), mean bias error (MBE), and root-mean-square error (RMSE) were 0.985, 0.027, and 0.0007, respectively. The detailed statistical analysis of the results is presented in Table 2 (regime 2 corresponds to the regime where the product sample is dried in the drying chamber).

CONCLUSIONS

The methods of solar drying were described, and the data on the structure and classification of different solar drying facilities were provided.

The mathematical model of the produce drying process in the offered recirculating solar drying facility was introduced. The experimental verification of the mathematical model for the recirculating solar power plant was presented.

Table 2. Accuracy of the mathematical model for kinetics of apple drying in open air solar drying and in a solar drying chamber

Model	Drying regime	k_m, h^{-1}	k_e, h^{-1}	n	a	R^2	RMSE	MBE
$MR = \exp(-kt)$	Regime 1	0.2372		—	—	0.939	0.053	0.0028
	Regime 2	0.3343		—	—	0.973	0.036	0.0013
$MR = \exp(-kt^n)$	Regime 1	1.284	0.143	0.828	—	0.950	0.048	0.0023
	Regime 2	0.1838	0.320	1.063	—	0.974	0.036	0.0013
$MR = a \exp(-kt)$	Regime 1	0.192		—	0.818	0.984	0.027	0.0007
	Regime 2	0.301		—	0.894	0.985	0.027	0.0007

As initial data, we used the changes in the ambient temperature and flux density of incident total solar radiation over several days.

The results of the statistical analysis of the diurnal variations in the temperature inside the solar dryer demonstrated good fit. In addition, the experimental verification of the known models of apple drying in the recirculating solar drying facility and in the open air were presented. Among these models, the Henderson and Pabis model illustrated the best fit between the estimated and experimental results. For further studies during the full-scale calculations, the Henderson and Pabis model of drying will be sufficient.

ACKNOWLEDGMENTS

We are grateful to our colleagues from the Physical–Technical Institute NGO Physics–Sun, Academy of Sciences of the Republic of Uzbekistan and the National Scientific Technical Institute of Renewable Energy Sources under the Uzbekistan Ministry of Energy for their continuous support.

REFERENCES

- Janjai, S., Solar drying technology, *Food. Eng. Rev.*, 2012, vol. 4, pp. 16–54.
- Pangavhane, D.R., Sawhney, R.L., and Sarsavadia, P.N., Design development and performance testing of a new natural convection solar dryer, *Energy*, 2002, vol. 27, pp. 579–590.
- Tembo, L., Chiteka, Z.A., Kadzere, I., Akinnifesi, F.K., and Tagwira, F., Blanching and drying period affect moisture loss and vitamin C content in *Ziziphus mauritiana* (Lamk.), *Afr. J. Biotechnol.*, 2008, vol. 8, pp. 3100–3106.
- Esper, A. and Muhlbauer, W., Solar drying—an effective means of food preservation, *Renewable Energy*, 1998, vol. 15, pp. 95–100.
- Ekechukwu, O.V. and Norton, B., Review of solar-energy drying systems II an overview of solar drying technology, *Energy Convers. Manage.*, 1999, vol. 40, pp. 615–655.
- Leon, M.A., Kumar, S., and Bhattacharya, S.C., A comprehensive procedure for performance evaluation of solar food dryers, *Renewable Sustainable Energy Rev.*, 2002, vol. 6, pp. 367–393.
- Purohit, P., Kumar, A., and Kandpal, T.C., Solar drying vs. open sun drying: a framework for financial evaluation, *Sol. Energy*, 2006, vol. 80, pp. 1568–1579.
- Leon, M.A., Kumar, S., and Bhattacharya, S.C., A comprehensive procedure for performance evaluation of solar food dryers, *Renewable Sustainable Energy Rev.*, 2002, vol. 6, pp. 367–393.
- Umarov, G.G., Solar dryer of vegetable agricultural products: Substantiation of process parameters and development of efficient solar plants, *Doctoral (Eng.) Dissertation*, Ashgabat, 1989.
- Khairiddinov, B.E., Development, research and implementation of a dryer solar greenhouse with a subsoil heat accumulator, *Doctoral (Eng.) Dissertation*, Ashgabat, 1990.
- Umarov, G.G., Mirziyaev, Sh.M., and Yusupbekov, O.N., *Geliosushka sel'khozproduktov* (Solar Drying of Agricultural Products), Tashkent, 1995.
- Ekechukwu, O.V. and Norton, B., Review of solar-energy drying systems II: An overview of solar drying technology, *Energy Convers. Manage.*, 1999, vol. 40, no. 6, pp. 615–655.
- Belessiotis, V. and Delyannis, E., Solar drying, *Sol. Energy*, 2011, vol. 85, pp. 1665–1691.
- Fudholi, A., Sopian, K., Ruslan, M.H., Alghoul, M.A., and Sulaiman, M.Y., Review of solar dryers for agricultural and marine products, *Renewable Sustainable Energy Rev.*, 2010, vol. 14, pp. 1–30.
- Sontakke, M.S. and Salve, S.P., Solar drying technologies: A review, *Int. Refereed J. Eng. Sci. (IRJES)*, 2015, vol. 4, no. 4, pp. 29–35.
- Vijaya Venkata Raman, S., Iniyani, S., and Goic, R., A review of solar drying technologies, *Renewable Sustainable Energy Rev.*, 2012, vol. 16, pp. 2652–2670.
- Ekechukwu, O.V. and Norton, B., Review of solar-energy drying systems III: Low temperature air-heating solar collectors for crop drying applications, *Energy Convers. Manage.*, 1999, vol. 40, no. 6, pp. 657–667.
- Sharma, A., Chen, C.R., Lan, N.V., Solar-energy drying systems: A review, *Renewable Sustainable Energy Rev.*, 2009, vol. 13, pp. 1185–1210.
- Mustayen, A.G.M.B., Mekhilef, S., and Saidur, R., Performance study of different solar dryers: A review, *Renewable Sustainable Energy Rev.*, 2014, vol. 34, pp. 463–470.
- Toshniwal, U. and Karale, S.R., A review paper on solar dryer, *Int. J. Eng. Res. Appl. (IJERA)*, 2013, vol. 3, no. 2, pp. 896–902.
- El-Sebaili, A.A. and Shalaby, S.M., Solar drying of agricultural products: A review, *Renewable Sustainable Energy Rev.*, 2012, vol. 16, pp. 37–43.
- Phadke, P.C., Walke, P.V., and Kriplani, V.M., A review on indirect solar dryers, *ARN J. Eng. Appl. Sci.*, 2015, vol. 10, no. 8, pp. 3360–3371.
- Jairaj, K.S., Singh, S.P., and Srikant, K., A review of solar dryers developed for grape drying, *Sol. Energy*, 2009, vol. 83, pp. 1698–1712.
- Reyes, A., Mahn, A., and Vásquez, F., Mushroom's dehydration in a hybrid-solar dryer, using a phase change material, *Energy Convers. Manage.*, 2014, vol. 83, pp. 241–248.
- Nabikhanov, B.M., Intensification of the process of solar drying of apples and grapes with discrete ventilation, *Cand. Sci. (Eng.) Dissertation*, Tashkent, 1990.
- Nazarov, M.R., Development and study of the effectiveness of a pilot-production radiation-convective solar drying plant for fruits and berries, *Cand. Sci. (Eng.) Dissertation*, Tashkent, 1998.
- Toirov, Z., Combined solar plant for drying fruits and grapes, *Geliotekhnika*, 1982, no. 1, p. 61.
- Il'yasov, S.G., et al., Thermoradiation-convective drying of grapes with preliminary treatment with IR radiation

- tion, *Izv. Vyssh. Uchebn. Zaved. Pishch. Tekhnol.*, 1989, no. 3, pp. 107–110.
29. Chua, K.J. and Chou, S.K., Low cost drying for developing countries, *Food Sci. Technol.*, 2003, vol. 14, pp. 519–528.
 30. Muhlbauer, W. and Muller, J., *Drying Atlas*, Cambridge, UK: Woodhead Publishing, 2020.
 31. Oueslati, H., Mabrouk, S.B., and Mami, A., Thermal modeling of solar dryer—numerical simulation, analysis and performance evaluation, *Int. J. Air-Cond. Refrig.*, 2018, vol. 26, no. 4, p. 1850032.
 32. Goyal, R.K. and Tiwari, G.N., Parametric study of a reverse flat plate absorber cabinet dryer: A new concept, *Sol. Energy*, 1997, vol. 60, no. 1, pp. 41–48.
 33. Kobayashi, K. and Salam, M.U., Comparing simulated and measured values using mean squared deviation and its components, *Agron. J.*, 2000, vol. 92, no. 2, pp. 345–352.
 34. Fontaine, J. and Ratti, C., Lumped-parameter approach for prediction of drying kinetics in foods, *J. Food Process. Eng.*, 1999, vol. 22, pp. 287–305.
 35. Lewis, W.K., The rate of drying of solid materials, *Ind. Eng. Chem.*, 1921, vol. 3, no. 5, pp. 427–432.
 36. Diamante, L.M. and Munro, P.A., Mathematical modelling of the thin layer solar drying of sweet potato slices, *Sol. Energy*, 1993, vol. 51, no. 4, pp. 271–276.
 37. Henderson, S.M., Progress in developing the thin layer drying equation, *Trans. ASAE*, 1974, vol. 17, pp. 1167–1172.
 38. Nazarov, M.R., et al., Compact solar dryer with active ventilation, *Mezhdunarodnaya nauchno-prakticheskaya konferentsiya “Solnechnaya energetika”* (International Scientific and Practical Conference “Solar Energy”), Tashkent, December 20–22, 2019.
 39. *Spravochnik po teploobmennikam (Reference Book on Heat Exchangers)*, Moscow: Energoatomizdat, 1987, vols. 1–2.

Translated by L. Mukhortova

SPELL: 1. OK